Clinical Biomechanics 49 (2017) 56–63

Contents lists available at ScienceDirect

Clinical Biomechanics

journal homepage: www.elsevier.com/locate/clinbiomech

The effects of prosthetic foot stiffness on transtibial amputee walking mechanics and balance control during turning

Courtney E. Shell[a], Ava D. Segal[b], Glenn K. Klute[b,c], Richard R. Neptune[a,*]

[a] Department of Mechanical Engineering, The University of Texas at Austin, Austin, TX 78712, USA
[b] Department of Veterans Affairs, Puget Sound Health Care System, Seattle, WA 98108, USA
[c] Department of Mechanical Engineering, University of Washington, Seattle, WA 98105, USA

ARTICLE INFO

Keywords:
Below-knee amputee
Biomechanics
Dynamic balance control
Energy storage and return prosthesis
Gait

ABSTRACT

Background: Little evidence exists regarding how prosthesis design characteristics affect performance in tasks that challenge mediolateral balance such as turning. This study assesses the influence of prosthetic foot stiffness on amputee walking mechanics and balance control during a continuous turning task.

Methods: Three-dimensional kinematic and kinetic data were collected from eight unilateral transtibial amputees as they walked overground at self-selected speed clockwise and counterclockwise around a 1-meter circle and along a straight line. Subjects performed the walking tasks wearing three different ankle-foot prostheses that spanned a range of sagittal- and coronal-plane stiffness levels.

Findings: A decrease in stiffness increased residual ankle dorsiflexion (10–13°), caused smaller adaptations (< 5°) in proximal joint angles, decreased residual and increased intact limb body support, increased residual limb propulsion and increased intact limb braking for all tasks. While changes in sagittal-plane joint work due to decreased stiffness were generally consistent across tasks, effects on coronal-plane hip work were task-dependent. When the residual limb was on the inside of the turn and during straight-line walking, coronal-plane hip work increased and coronal-plane peak-to-peak range of whole-body angular momentum decreased with decreased stiffness.

Interpretation: Changes in sagittal-plane kinematics and kinetics were similar to those previously observed in straight-line walking. Mediolateral balance improved with decreased stiffness, but adaptations in coronal-plane angles, work and ground reaction force impulses were less systematic than those in sagittal-plane measures. Effects of stiffness varied with the residual limb inside versus outside the turn, which suggests that actively adjusting stiffness to turn direction may be beneficial.

1. Introduction

Appropriate prescription of prosthetic components plays a critical role in successful rehabilitation outcomes for lower-limb amputees. While studies have investigated the influence of prosthetic foot design characteristics on amputee straight-line walking (Fey et al., 2011; Major et al., 2014; Ventura et al., 2011a; Zelik et al., 2011), few studies have investigated these effects in other mobility tasks such as turning. Turning can account for as much as 45% of steps in a given task (Glaister et al., 2007), and thus plays a prominent role in activities of daily living.

Non-amputees execute turns differently than amputees. For non-amputees, mediolateral ground reaction force (GRF) impulses oscillate the center of mass (CoM) between support legs during straight-line walking and are modified to accelerate the body around a turn (Glaister et al., 2008; Orendurff et al., 2006). Non-amputees also lean into turns, which shifts the CoM over or even lateral of the inside limb during the turn (Orendurff et al., 2006). In contrast, unilateral transtibial amputees have a decreased lateral GRF impulse from the inside limb (Segal et al., 2011; Ventura et al., 2011b) and keep their CoM more centered over their base of support (Segal et al., 2011), which may be a strategy they use to decrease their risk of falling.

Despite these adaptations, amputees are less stable than non-amputees during turning (Segal et al., 2010) and the residual limb contributes less to balance control than the intact limb (Curtze et al., 2012). Previous studies have found that decreased regulation of whole-body angular momentum is associated with an increase in falls and a decrease in clinical balance measures (e.g., Nott et al., 2014; Pijnappels et al., 2005). In straight-line walking and stair climbing, amputees have a larger range of angular momentum than non-amputees (Pickle et al.,

* Corresponding author at: Department of Mechanical Engineering, The University of Texas at Austin, 1 University Station C2200, Austin, TX 78712, USA.
E-mail address: rneptune@mail.utexas.edu (R.R. Neptune).

http://dx.doi.org/10.1016/j.clinbiomech.2017.08.003
Received 10 November 2016; Accepted 13 August 2017

2014; Sheehan et al., 2015; Silverman and Neptune, 2011), which suggests they have decreased balance control. Further research has shown that there is a correlation between prosthetic foot stiffness and the ability to regulate balance in response to perturbations during quiet stance (Nederhand et al., 2012). Therefore, careful stiffness selection may provide an effective mechanism to improve amputee balance during turning tasks.

Previous studies of straight-line walking have shown that sagittal-plane foot stiffness can be used to modulate prosthetic foot contributions to body support and forward propulsion, with more compliant feet allowing greater ankle range of motion and energy storage and return (e.g., Fey et al., 2011; Zelik et al., 2011). However, no study has investigated these effects during turning. Significant differences in ankle kinematics and kinetics between straight-line walking and turning exist in the coronal plane for non-amputees (Jenkyn et al., 2010). Thus, prosthesis characteristics that influence movement and energy flow in the coronal plane are also likely to affect turning in amputees. In addition, while non-amputees modulate coronal-plane hip joint work to control a turn, amputees modulate sagittal-plane hip joint work (Ventura et al., 2011b). This difference in work modulation highlights a different turning strategy used by amputees, which may be due to non-optimal prosthesis stiffness characteristics and limited forward and mediolateral propulsion from the prosthetic ankle. Thus, a better understanding of the influence of sagittal- and coronal-plane stiffness on generation of mediolateral propulsion is needed to better inform the prescription of prostheses that improve amputee turning ability.

While controlled stiffness manipulation of commercially available carbon fiber prosthetic feet is difficult, additive manufacturing processes such as selective laser sintering (SLS) are well-suited for manufacturing ankles of different stiffness levels as they facilitate controlled modification of design parameters, allow for geometric complexity and produce fully functional prototypes. SLS has previously been used to successfully manufacture prosthetic sockets (Faustini et al., 2006), ankle-foot orthoses (Faustini et al., 2008; Harper et al., 2014; Schrank and Stanhope, 2011), prosthetic feet (Fey et al., 2011; South et al., 2010) and ankles (Ventura et al., 2011a).

In this study, both prosthetic foot sagittal- and coronal-plane stiffness levels were simultaneously varied to assess their influence on walking mechanics and balance control during turning. We expected that as prosthetic foot stiffness is decreased, peak ankle angles and ankle work will increase in the sagittal and coronal planes, which will help normalize turning mechanics and improve balance control.

2. Methods

2.1. Modification of prosthesis stiffness

A low-profile version of a commonly prescribed carbon fiber prosthetic foot (Category 9, LP Vari-Flex® with EVO™, Össur, Reykjavik, Iceland) was combined in series with custom SLS-manufactured ankles. Three prosthetic ankles (compliant, intermediate and stiff) were manufactured from Nylon 11 (PA D80-ST, Advanced Laser Materials, Temple, TX, USA) using SLS (Vanguard HiQ/HS Sinterstation, 3D Systems Corporation, Rock Hill, SC, USA) to create a set of ankle-foot combinations that span a range of stiffness levels. Stiffness was modified by changing the ankle thickness and moment arm length of the C-shaped ankle and characterized by loading the ankle-foot combinations to 1000 N in static compression (Fig. 1, Instron Model 3345, Norwood, MA, USA). Two positions were tested, emulating foot-flat without a cosmesis at 0° and 5° eversion. The stiffness when tested at 0° eversion represented the sagittal-plane stiffness while the test at 5° eversion represented the coronal-plane stiffness. Ankle stiffness levels ranged from 69 to 112 N/mm in the sagittal plane and 63 to 106 N/mm in the coronal plane. The stiff ankle had a stiffness similar to that of a Vari-Flex® with EVO™ Category 5 stiffness foot (Össur, Reykjavik, Iceland), which had stiffness levels of 118 N/mm and 106 N/mm in the sagittal and coronal planes, respectively. Compared to the stiff combination, the intermediate and compliant combinations were ~15% and 40% less stiff, respectively, in the sagittal plane and ~20% and 40% less stiff, respectively, in the coronal plane.

2.2. Human subject testing

Eight unilateral transtibial amputees (Table 1) completed an IRB-approved protocol of straight-line walking and turning maneuvers with each of the three ankles in random order. All subjects wore a prosthesis for at least 4 h per day and could ambulate without upper extremity aides. Differences in mass between the ankle-foot combinations were normalized by adding small weights inside the cosmesis when the lighter combinations were tested. After fitting and aligning the foot by a certified prosthetist, subjects acclimated to each ankle-foot until they felt comfortable.

Subjects walked at their self-selected speed clockwise and counter-clockwise around a 1-meter-radius circle across up to six force plates (Advanced Mechanical Technology, Inc., Watertown, MA, USA; Kistler Instrument Corporation, Amherst, NY, USA). In addition, each subject

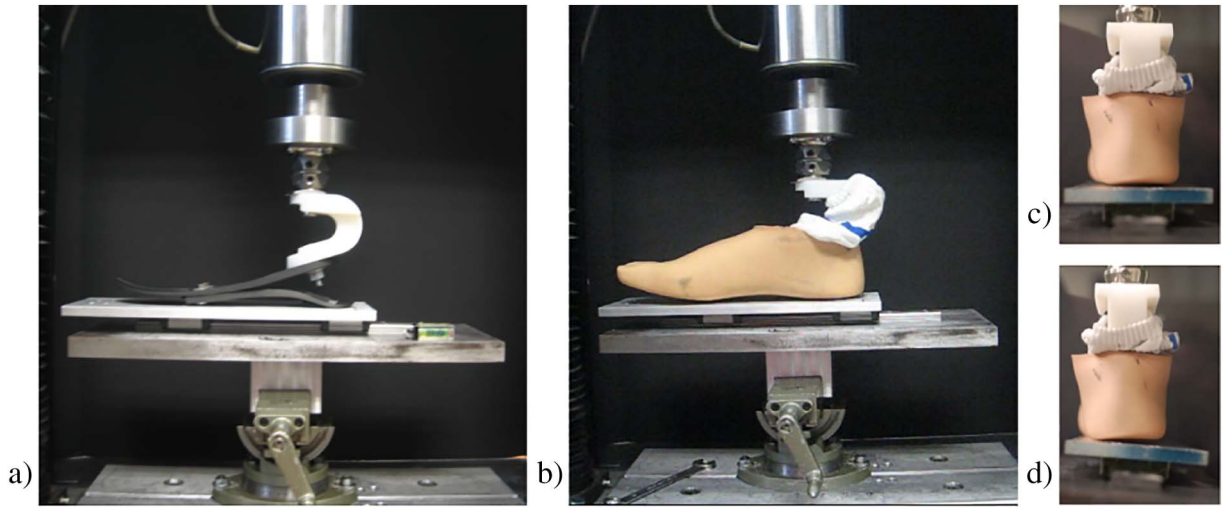

Fig. 1. (a) After aligning foot-flat without the cosmesis, (b) ankle-foot combinations with the cosmesis were loaded to 1000 N in compression at foot-flat with the foot at (c) 0° eversion and (d) 5° eversion.

Table 1
Subject characteristics.

	Age (years)	Mass (kg)	Height (m)	Years since amputation	Gender	Residual limb	Etiology	Prescribed foot
A01	45	86.8	1.80	18.0	M	Left	Infection	Ossur Vari-Flex®
A02	27	76.4	1.83	2.8	M	Left	Trauma	Endolite Elite Blade
A03	34	69.9	1.79	11.0	M	Left	Trauma	Ossur Vari-Flex® with EVO
A04	30	76.7	1.79	3.0	M	Right	Trauma	Ossur Re-Flex Rotate™ VSP
A05	67	65.5	1.74	11.0	M	Right	Trauma	Ottobock Triton Harmony®
A06	23	65.9	1.81	2.9	M	Right	Trauma	Fillauer Wave Sport
A07	52	81.8	1.65	5.0	M	Left	Trauma	Ossur Vari-Flex®
A08	61	86.8	1.78	7.5	M	Right	Trauma	College Park Trustep®
Avg	42	76.2	1.77	7.7				
SD	15	8.1	0.05	5.0				

performed straight-line walking overground on a 10-meter walkway with five embedded force plates at their self-selected speed. Repeated trials were collected for each ankle to obtain clean force plate strikes in at least four trials per foot.

GRF and marker data were collected at 1200 Hz and 120 Hz, respectively, using a 12-camera motion capture system (Vicon Nexus, Vicon Motion Systems, Oxford, UK). Forty-one 14-mm reflective markers were placed on the head (4 markers), then one each on the C7 vertebra, T10 vertebra, right scapula, jugular notch of the sternum, and xiphoid process consistent with the Vicon Plug-in Gait marker set, and bilaterally on the acromion, lateral epicondyle of the elbow, radial and ulnar styloid processes, third metacarpal head, anterior and posterior superior iliac spine, greater trochanter, lateral and medial epicondyles of the knee, lateral and medial malleoli, first and fifth metatarsal heads, dorsal foot and heel. Clusters of four markers were also placed bilaterally on the thigh and shank. Residual limb markers were placed symmetrically with the intact limb markers. The medial knee, medial malleolus and first metatarsal head markers were removed after the static calibration trial to allow subjects more freedom of movement.

2.3. Data analysis

The effect of stiffness on walking mechanics was assessed via joint angles, joint powers and GRF impulses. The effect of stiffness on dynamic balance was assessed via whole-body angular momentum in the sagittal and coronal planes.

Experimental data were processed using Visual3D (C-Motion, Inc., Germantown, MD, USA). Functional movement trials were used to find hip functional joint centers and knee functional joint axes (Schwartz and Rozumalski, 2005). The mass of the residual shank was half that of the intact shank (Mattes et al., 2000). The residual shank center of mass was located below the knee a distance equal to 25% of the shank length (Mattes et al., 2000; McConville et al., 1980), which was calculated as the distance between the markers at the knee axis and the malleoli. GRF and marker data were filtered using a 4th-order, low-pass Butterworth filter with cutoff frequencies of 20 and 6 Hz, respectively. For the turning trials, GRFs were defined with respect to a rotating reference frame with the origin located at the center of the 1-meter circle, with the positive x-axis through the subject's CoM projected on the floor, the y-axis tangent to the circular path and the z-axis extending upward out of the floor. Joint angles and powers were calculated and time-normalized to the gait cycle. GRFs were normalized by the subject's body weight. Joint powers were normalized by subject mass. In addition, the average residual ankle angle during the first 90% of swing was subtracted from the residual ankle joint angle across the gait cycle so that the reported angles were relative to an unloaded value. Whole-body angular momentum ($\overline{H}$) was calculated about the body CoM as:

$$\overline{H} = \sum_{i=1}^{n} [\overline{r}_{iCoM\ to\ bodyCoM} \times m_i \overline{v}_{iCoM\ to\ bodyCoM} + I_i \overline{\omega}_i], \quad (1)$$

where $\overline{r}_{iCoM\ to\ bodyCoM}$ and $\overline{v}_{iCoM\ to\ bodyCoM}$ are the position and velocity of the i^{th} segment's center of mass relative to the body CoM, respectively, and $\overline{\omega}_i$, m_i, and I_i are the angular velocity, mass, and moment of inertia of i^{th} segment, respectively. Angular momentum was normalized by body height (m) and mass (kg).

Data analysis was performed using MATLAB (The MathWorks, Inc., Natick, MA, USA). Positive and negative joint work and GRF impulses were calculated as the time-integral of the positive and negative joint power and GRFs, respectively, across the entire gait cycle. Joint work was also calculated in three regions of the gait cycle: swing and the first and second halves of stance. Peak-to-peak range of whole-body angular momentum was calculated for early and late stance as well as early and late swing in the sagittal plane and for stance and swing in the coronal plane. The effects of ankle stiffness on walking mechanics during the different walking tasks (leg on the inside of a turn, leg on the outside of a turn and straight-line walking) for the residual and intact limbs were examined using a linear mixed-effects model (SPSS Statistics 23, IBM Corp., Armonk, NY, USA). The model included fixed-effects terms for three factors (ankle, task, leg), a covariate (speed) and four factorial interactions (ankle∗leg, ankle∗task, task∗leg, and ankle∗leg∗task). The effects of ankle stiffness on dynamic balance during the different walking tasks were also examined using a linear mixed-effects model. The model included fixed-effects terms for two factors (ankle, task), a covariate (speed) and a factorial interaction (ankle∗task). For walking mechanics and dynamic balance, the linear mixed-effects models included random-effects terms for the intercept and speed by subject. Significant main effects as well as two-way interaction effects involving the ankle factor were examined with Bonferroni-corrected post-hoc pairwise comparisons ($\alpha = 0.05$). With a few exceptions, only effects involving the ankle are reported. Tables of *p*-values for main and interaction effects as well as mean differences, standard errors and *p*-values for pairwise comparisons are available in the Supplementary Material.

3. Results

We examined the effects of ankle stiffness on joint angles, joint work, GRF impulses and angular momentum during turning and straight-line walking. Unless otherwise specified, all statements about biomechanical quantities apply to both the residual and intact legs. Statistical analyses of the biomechanical quantities used speed as a covariate. Across the three ankle stiffnesses, average self-selected walking speed was 0.80 and 0.79 m/s with the residual limb inside and outside of the turn, respectively, and 1.25 m/s during straight-line walking. Across the walking tasks, average self-selected walking speed was 0.93, 0.96, and 0.95 m/s with the compliant, intermediate and stiff ankle, respectively. For individual subjects, the difference in average walking speed with each of the three ankle stiffnesses during the three walking tasks ranged from 1% to 14% of the average walking speed in that task and averaged 6% across the eight subjects.

Table 2
Mean (standard deviation) peak sagittal-plane hip, knee and ankle angles for the residual (Res) and intact (Int) limbs when the leg was on the inside (In) and outside (Out) of the turn as well as during straight-line walking at self-selected speed (Str) while the subject was wearing the compliant, intermediate and stiff ankles. Significant ankle main effects (†) as well as leg∗ankle (ℓ) and task∗ankle (§) interaction effects are indicated in addition to significant pairwise differences between the compliant and intermediate (□), compliant and stiff (■) and the intermediate and stiff (■) ankles. In addition, shading highlights significant leg∗ankle interactions and bolded text highlights significant task∗ankle interactions.

Peak Angle (°)	Task	Leg	Compliant	Intermediate	Stiff
			Mean (SD)	Mean (SD)	Mean (SD)
Hip Extension (Stance) †■■ Res: ℓ□■■ Int: ℓ■	In	Res	-10.9 (3.0)	-11.8 (3.6)	-12.6 (4.1)
		Int	-13.9 (5.1)	-13.3 (5.2)	-15.4 (4.3)
	Out	Res	-10.0 (3.1)	-10.9 (2.5)	-12.7 (3.9)
		Int	-12.1 (3.5)	-11.5 (3.5)	-12.2 (3.6)
	Str	Res	-13.7 (3.8)	-15.4 (2.4)	-16.3 (3.4)
		Int	-17.3 (4.5)	-16.8 (4.1)	-17.6 (4.3)
Hip Flexion (Swing) †□■■ Res: ℓ□■■ Int: ℓ□■■	In	Res	28.6 (4.1)	28.5 (3.7)	27.2 (4.2)
		Int	23.4 (4.1)	20.5 (5.7)	20.4 (5.0)
	Out	Res	25.5 (4.0)	25.0 (3.9)	23.9 (3.7)
		Int	21.9 (4.3)	20.1 (4.7)	18.9 (4.7)
	Str	Res	29.8 (2.1)	28.2 (2.7)	27.5 (1.9)
		Int	24.8 (4.4)	23.7 (4.4)	22.8 (3.9)
Knee Flexion (Swing) †□■ Res: ℓ□■ Int: ℓ□■	In	Res	-68.9 (4.3)	-66.2 (5.5)	-64.8 (7.2)
		Int	-64.6 (5.1)	-61.8 (6.0)	-63.0 (5.7)
	Out	Res	-69.6 (6.2)	-67.1 (5.4)	-66.4 (6.2)
		Int	-63.1 (4.4)	-60.2 (11.6)	-60.4 (9.3)
	Str	Res	-75.9 (3.8)	-71.9 (5.0)	-70.5 (4.9)
		Int	-66.8 (4.9)	-65.8 (4.0)	-65.5 (4.1)
Ankle Plantarflexion (Early Stance) †□■■ Res: ℓ■■ Int: ℓ□■	In	Res	**-3.8 (1.7)**	**-4.4 (1.5)**	**-4.9 (1.9)**
	§□■	Int	**-6.8 (3.1)**	**-8.7 (3.0)**	**-8.7 (2.4)**
	Out	Res	**-4.4 (1.2)**	**-4.2 (1.3)**	**-5.3 (1.5)**
	§□■	Int	**-6.1 (2.5)**	**-7.8 (3.0)**	**-7.1 (2.7)**
	Str	Res	**-5.7 (1.4)**	**-5.4 (1.4)**	**-6.2 (1.7)**
	§□■■	Int	**-6.6 (2.1)**	**-8.2 (2.2)**	**-8.8 (1.2)**
Ankle Dorsiflexion (Late Stance) †□■■ Res: ℓ□■■ Int: ℓ□■■	In	Res	**21.0 (4.6)**	**11.6 (2.5)**	**9.1 (2.2)**
	§□■■	Int	**13.2 (4.1)**	**12.0 (3.6)**	**11.2 (3.9)**
	Out	Res	**19.3 (3.7)**	**11.8 (2.1)**	**9.2 (2.5)**
	§□■■	Int	**9.0 (3.3)**	**6.7 (3.6)**	**6.8 (3.3)**
	Str	Res	**23.3 (2.7)**	**13.8 (1.9)**	**10.4 (2.2)**
	§□■■	Int	**11.5 (3.1)**	**9.3 (4.0)**	**8.9 (3.7)**

3.1. Joint angles

In the sagittal plane, peak hip flexion, knee flexion and ankle dorsiflexion increased with a decrease in stiffness while peak hip extension and early-stance plantarflexion decreased (Table 2; HIP FLEXION: $p \leq 0.002$; KNEE FLEXION: $p \leq 0.002$; ANKLE DORSIFLEXION: $p \leq 0.046$; HIP EXTENSION: $p \leq 0.001$; ANKLE PLANTARFLEXION: $p \leq 0.041$).

In the coronal plane, peak hip adduction during early stance when the limb was on the inside of a turn (task∗ankle effect and compliant vs. intermediate $p = 0.001$) and late stance (ankle effect $p = 0.037$, compliant vs. intermediate $p = 0.031$) was greater with the intermediate ankle but peak hip abduction in swing was greatest with the compliant ankle (Table 3; ankle effect and pairwise comparisons $p \leq 0.019$; task∗ankle effect and In/Straight pairwise comparisons $p \leq 0.028$). Late-stance peak intact ankle inversion increased with a decrease in stiffness (Table 3; leg∗ankle effect $p = 0.034$, Intact pairwise comparisons $p = 0.000$). No significant differences were observed in peak ankle eversion with changes in ankle stiffness.

3.2. Joint work

Positive sagittal-plane hip work decreased with decreasing ankle stiffness in the residual limb but increased in the intact limb (Fig. 2; $p \leq 0.025$). Negative sagittal-plane knee work, intact positive sagittal-plane knee work and residual positive sagittal-plane ankle work increased with a decrease in stiffness (Fig. 2; POSITIVE SAGITTAL KNEE: $p \leq 0.007$; NEGATIVE SAGITTAL KNEE: $p = 0.000$; POSITIVE SAGITTAL ANKLE: $p \leq 0.012$). Some of these trends are more readily apparent if work is examined in early stance, late stance and swing instead of across the whole gait cycle (Supplementary material, Fig. S1). Negative sagittal-plane ankle work was highest with the intermediate ankle (Fig. 2; $p \leq 0.001$). Residual limb positive sagittal-plane hip work was higher than that of the intact limb when the residual limb was on the inside of the turn but lower when the residual limb was on the outside of the turn (leg∗task effect and pairwise comparisons $p = 0.000$).

Positive coronal-plane hip work increased with a decrease in ankle stiffness when the leg was on the inside of a turn and during straight-line walking (Fig. 3; $p \leq 0.004$) while negative coronal-plane hip work decreased in the residual limb during turning (Fig. 3; leg∗ankle effect and Residual pairwise comparisons $p \leq 0.006$; task∗ankle effect and In/Out pairwise comparisons $p \leq 0.017$). These changes generally occurred during late stance (Supplementary material, Fig. S2). Altering ankle stiffness affected the anteroposterior and vertical GRF impulses but had little effect on the mediolateral GRF impulses (Fig. 4). The inward GRF impulse decreased with a decrease in stiffness when the limb was on the outside of the turn ($p \leq 0.001$). Across all tasks, the residual limb anterior (propulsive) GRF impulse ($p \leq 0.012$) and the intact limb posterior (braking) GRF impulse ($p \leq 0.003$) increased with a decrease in stiffness. The vertical GRF impulse was lower with the compliant compared to the intermediate and stiff ankles in the residual

Table 3
Mean (standard deviation) peak coronal-plane hip and ankle angles for the residual (Res) and intact (Int) limbs when the leg was on the inside (In) and outside (Out) of the turn as well as during straight-line walking at self-selected speed (Str) while the subject was wearing the compliant, intermediate and stiff ankles. Significant ankle main effects (†) as well as leg∗ankle (ℓ) and task∗ankle (§) interaction effects are indicated in addition to significant differences between the compliant and intermediate (□), compliant and stiff (■) and the intermediate and stiff (■) ankles. In addition, shading highlights significant leg∗ankle interactions and bolded text highlights significant task∗ankle interactions.

Peak Angle (°)	Task	Leg	Compliant	Intermediate	Stiff
			Mean (SD)	Mean (SD)	Mean (SD)
Hip Adduction (Early Stance) †■	In	Res	**7.9 (4.3)**	**9.3 (3.5)**	7.8 (4.3)
	§□	Int	**4.4 (2.7)**	**5.5 (2.7)**	5.0 (3.0)
	Out	Res	**3.6 (4.4)**	4.2 (4.3)	**2.9 (4.6)**
	§■	Int	**-0.1 (4.4)**	-1.0 (5.5)	**-1.9 (5.9)**
	Str	Res	7.1 (3.3)	6.7 (3.1)	6.7 (3.9)
		Int	4.5 (3.0)	3.8 (2.7)	3.3 (3.6)
Hip Adduction (Late Stance) †□	In	Res	6.5 (4.3)	8.1 (3.2)	6.9 (4.1)
		Int	2.2 (4.1)	3.7 (3.5)	3.5 (4.5)
	Out	Res	0.0 (5.2)	1.2 (4.6)	1.1 (5.1)
		Int	0.4 (5.5)	0.5 (5.9)	0.1 (5.2)
	Str	Res	5.9 (3.6)	5.4 (2.6)	5.4 (3.6)
		Int	2.2 (3.8)	2.6 (3.3)	1.8 (4.1)
Hip Abduction (Swing) †□■	In	Res	**-1.0 (3.9)**	**0.1 (4.1)**	**-0.6 (4.5)**
	§□■	Int	**-5.1 (3.4)**	**-2.9 (3.5)**	**-3.4 (3.6)**
	Out	Res	-6.8 (3.1)	-6.5 (3.0)	-7.6 (4.4)
		Int	-7.4 (4.4)	-7.7 (4.6)	-7.7 (4.3)
	Str	Res	**-5.1 (2.6)**	**-4.3 (2.8)**	**-3.7 (2.8)**
	§□■	Int	**-7.6 (3.8)**	**-6.0 (3.8)**	**-6.7 (4.0)**
Ankle Inversion (Late Stance) †□■ Int: ℓ□■	In	Res	-0.3 (0.8)	-0.7 (0.9)	-0.6 (0.8)
		Int	-1.8 (5.2)	-2.7 (5.1)	-3.5 (6.2)
	Out	Res	5.5 (1.6)	5.7 (1.4)	5.4 (1.3)
		Int	9.0 (3.1)	7.5 (3.5)	8.8 (3.7)
	Str	Res	1.6 (1.0)	1.0 (0.8)	1.3 (0.9)
		Int	1.6 (3.1)	0.7 (3.0)	0.4 (2.6)
Ankle Eversion (Late Stance)	In	Res	-3.2 (1.4)	-4.0 (2.0)	-3.5 (1.7)
		Int	-13.5 (5.6)	-14.1 (4.8)	-15.0 (4.2)
	Out	Res	1.2 (0.6)	1.1 (0.6)	1.3 (0.7)
		Int	-0.6 (3.4)	-1.3 (2.8)	-0.7 (2.7)
	Str	Res	-1.1 (1.2)	-1.4 (1.3)	-1.1 (1.4)
		Int	-7.4 (4.1)	-7.6 (2.7)	-7.6 (2.8)

limb but greater in the intact limb ($p \leq 0.007$).

3.3. Angular momentum

A decrease in ankle stiffness led to an increase in the peak-to-peak range of sagittal-plane whole-body angular momentum during late residual limb swing and early stance but a decrease during late stance and early swing (Fig. 5; LATE SWING: ankle effect and pairwise comparisons $p = 0.000$; task∗ankle interaction effect and pairwise comparisons Out/Straight $p \leq 0.001$; EARLY STANCE: ankle effect $p = 0.022$, intermediate vs. stiff $p = 0.043$; LATE STANCE: ankle effect and pairwise comparisons $p = 0.000$; task∗ankle interaction effect and pairwise comparisons Straight $p = 0.000$; EARLY SWING: ankle effect and pairwise comparisons $p \leq 0.005$; task∗ankle interaction effect $p = 0.000$, pairwise comparisons Out/Straight $p \leq 0.039$). During stance, the range of sagittal-plane angular momentum was lower when the residual limb was on the outside of the turn compared to the inside or straight-line walking (task effect and pairwise comparisons Out vs. In and Out vs. Straight $p = 0.000$). However, during swing, the range of sagittal-plane angular momentum was higher for the residual limb on the outside of the turn compared to the inside (EARLY SWING: task effect and pairwise comparison Out vs. In $p = 0.000$; LATE SWING: task effect and pairwise comparisons Out vs. In and Out vs. Straight $p = 0.000$). The peak-to-peak range of coronal-plane whole-body angular momentum decreased with decreasing stiffness during stance (ankle effect and pairwise comparisons $p \leq 0.017$; task∗ankle effect and In/Straight pairwise comparisons $p \leq 0.011$) and, when the residual limb was on the inside of the turn, during swing (Fig. 5; $p = 0.000$). During both stance and swing, the range of coronal-plane whole-body angular momentum was highest when the residual limb was on the inside of the turn, lowest during straight-line walking and intermediate when the residual limb was on the outside of the turn ($p = 0.000$).

4. Discussion

In order to assess the influence of prosthesis stiffness on walking mechanics and balance control during turning, amputees walked overground at their self-selected speed around a 1-meter circle with the residual limb on the inside and outside of the turn as well as in a straight line while wearing ankle-foot prostheses with different stiffness levels (compliant, intermediate and stiff). Our expectation that peak ankle angles and ankle work would increase in the sagittal and coronal planes with a decrease in stiffness was only partially supported. As expected, peak ankle dorsiflexion and, in the intact limb, inversion increased with a decrease in stiffness, but plantarflexion decreased and eversion was not significantly different. Positive residual limb sagittal-plane ankle work increased with a decrease in stiffness, but sagittal-plane negative ankle work was higher for the intermediate ankle while intact-limb positive and negative coronal-plane ankle work were lowest with the intermediate ankle.

Adaptations in sagittal-plane joint angles to changes in stiffness during the turning tasks were similar to those previously observed for straight-line walking (Fey et al., 2011), while coronal-plane adaptations were less systematic. Both the residual and intact legs were more flexed with less stiff ankles as they exhibited greater hip and knee flexion as well as ankle dorsiflexion. In the coronal plane, the intermediate compared to the compliant ankle resulted in greater hip adduction in

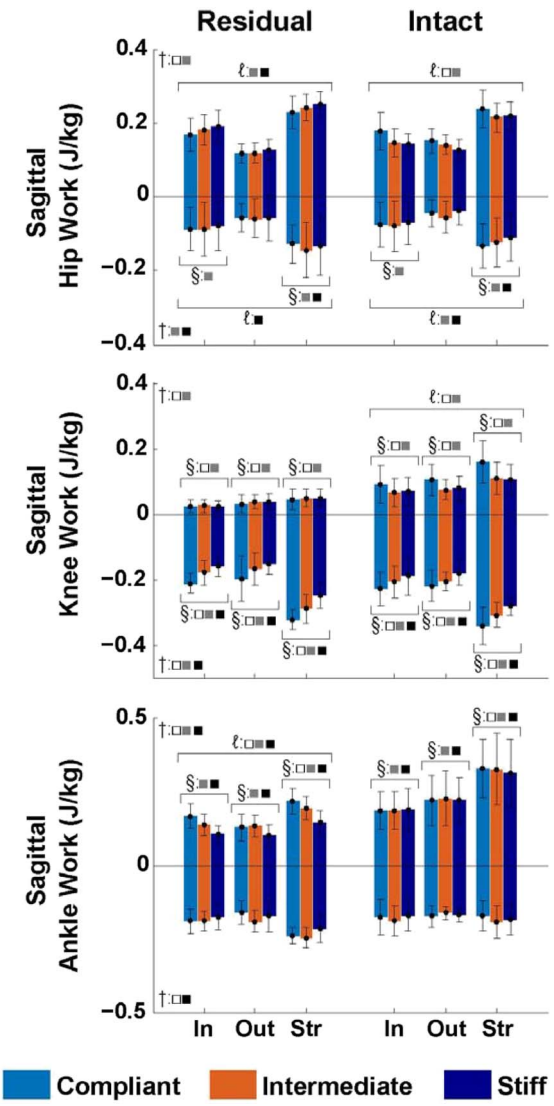

Fig. 2. Mean (standard deviation error bars) sagittal-plane hip, knee and ankle work for the residual and intact limbs on the inside (In) and outside (Out) of the turn as well as during straight-line walking at self-selected speed (Str) with the compliant, intermediate and stiff ankles. Significant ankle main effects (†) as well as leg∗ankle (ℓ) and task∗ankle (§) interaction effects are indicated in addition to significant differences between the compliant and intermediate (□), compliant and stiff (■) and the intermediate and stiff (■) ankles.

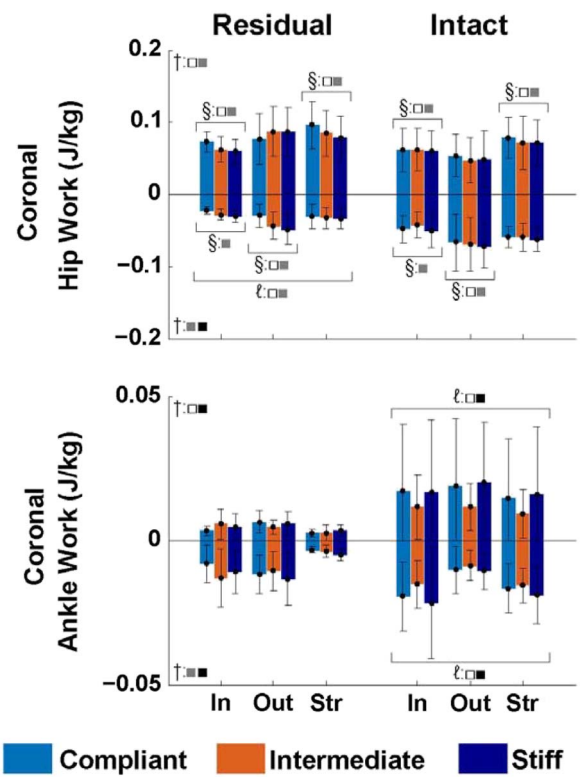

Fig. 3. Mean (standard deviation error bars) coronal-plane hip and ankle work for the residual and intact limbs on the inside (In) and outside (Out) of the turn as well as during straight-line walking at self-selected speed (Str) with the compliant, intermediate and stiff ankles. Significant ankle main effects (†) as well as leg∗ankle (ℓ) and task∗ankle (§) interaction effects are indicated in addition to significant differences between the compliant and intermediate (□), compliant and stiff (■) and the intermediate and stiff (■) ankles.

late stance and in early stance when the residual limb was on the inside of a turn as well as less hip abduction in swing. Decreased stiffness increased intact ankle inversion but did not affect eversion. As the ankle is primarily inverted when on the outside of the turn and everted when on the inside of the turn, changes in coronal-plane ankle angle with decreased stiffness impacted the leg that was on the outside of the turn the most. Variability in peak ankle eversion when the limb was on the inside of the turn was higher than that of ankle inversion when the limb was on the outside of the turn. This suggests that differences in individual subjects' turning strategy (i.e., the amount of ankle eversion used during a turn) may have overshadowed differences caused by a change in ankle stiffness. Thus, the change in stiffness led to small coronal-plane adaptations ($< 2.5^{\circ}$) at the hip as well as intact ankle inversion without significantly affecting ankle eversion.

The residual limb performed greater sagittal-plane hip work when on the inside of the turn than the intact limb did, consistent with a previous study of transtibial amputee turning (Ventura et al., 2011b). However, decreasing prosthesis stiffness diminished this difference as positive sagittal-plane hip work decreased in the residual limb and increased in the intact limb. Decreasing prosthesis stiffness also increased negative sagittal-plane knee work as well as intact positive sagittal-plane knee work. In the coronal plane, amputees have been shown to absorb and generate less residual hip power when the limb is on the inside of the turn and generate less intact hip power for the limb inside or outside of the turn compared to non-amputees (Ventura et al., 2011b). Decreasing prosthesis stiffness increased positive coronal-plane hip work when the limb was on the inside of the turn and decreased negative coronal-plane residual hip work when the limb was both inside and outside of the turn. Thus, as stiffness decreased, hip power generation increased to more closely resemble that of non-amputees but residual limb hip power absorption diverged more from that of non-amputees.

Decreasing ankle stiffness decreased residual limb vertical GRF impulses, increased residual limb propulsive GRF impulses, and increased intact limb braking GRF impulses, which is consistent with trends observed in peak GRFs and residual limb push-off work in previous studies (Fey et al., 2011; Major et al., 2014; Zelik et al., 2011). The outward (lateral) GRF impulse did not change with stiffness and only minor changes were observed in the inward (medial) GRF impulse when the leg was on the outside of the turn.

Peak-to-peak range of sagittal-plane whole-body angular momentum decreased with decreasing ankle stiffness in late-stance and early-swing, but was larger with the compliant ankle compared to the intermediate and stiff ankles in late-swing. During swing, the changes in sagittal-plane angular momentum due to stiffness were largest when the residual limb was on the outside of the turn and during straight-line walking. Compared to non-amputees, amputees have a higher range of

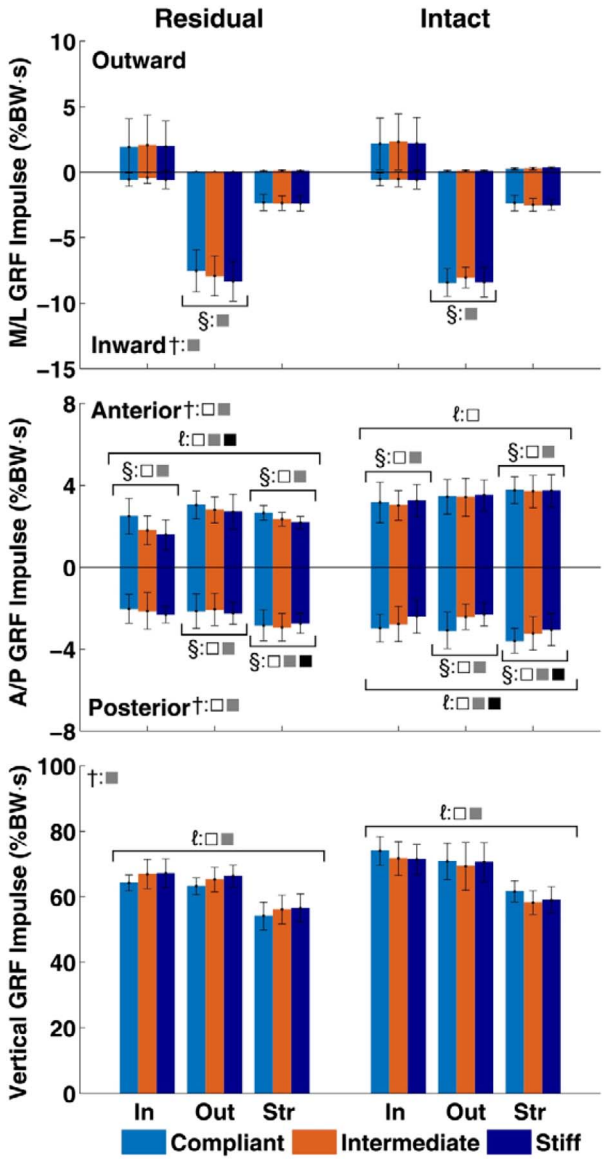

Fig. 4. Mean (standard deviation error bars) mediolateral (M/L), anteroposterior (A/P) and vertical ground reaction force (GRF) impulses for the residual and intact limbs on the inside (In) and outside (Out) of the turn as well as during straight-line walking at self-selected speed (Str) with the compliant, intermediate and stiff ankles. Significant ankle main effects (†) as well as leg∗ankle (ℓ) and task∗ankle (§) interaction effects are indicated in addition to significant differences between the compliant and intermediate (□), compliant and stiff (■) and intermediate and stiff (■) ankles.

sagittal-plane angular momentum during the first half of residual limb stance and a lower range during the second half of residual limb stance (Silverman and Neptune, 2011). Thus, changing the stiffness can help shift the range of sagittal-plane whole-body angular momentum to be more symmetrical like that of non-amputees. Although the residual limb was not in contact with the ground during residual limb swing, a change in prosthetic ankle stiffness caused changes in propulsion from the residual limb at push-off, which continues to affect whole-body angular momentum throughout swing. Previous work exploring amputee angular momentum during straight-line walking found that amputees had a lower range of sagittal-plane angular momentum during swing compared to non-amputees and correlated the decrease to lower peak propulsive GRFs from the residual limb compared to the non-amputee limb (Silverman and Neptune, 2011). In the present study, propulsive GRF impulses increased with a decrease in prosthesis stiffness, which may have contributed to the increase in the range of sagittal-plane angular momentum during late swing.

Decreasing ankle stiffness decreased stance peak-to-peak range of coronal-plane angular momentum, especially when the residual limb was on the inside of the turn and during straight-line walking. Swing peak-to-peak range in coronal-plane angular momentum also decreased with a decrease in stiffness when the residual limb was on the inside of the turn. Previous work has shown that there is a correlation between increased change in coronal-plane angular momentum and decreased clinical balance scores in hemiparetic subjects (Nott et al., 2014) and that amputees have an increased range of coronal-plane angular momentum compared to non-amputees (Sheehan et al., 2015; Silverman and Neptune, 2011). As a less stiff prosthesis decreased the peak-to-peak range of coronal-plane angular momentum, it may help amputees emulate non-amputee gait and improve balance control, especially during straight-line walking and when the residual limb is on the inside of the turn. As the time rate of change of whole-body angular momentum in the coronal plane is a function of the mediolateral and vertical GRFs and foot placement, and since few significant differences were found in the mediolateral GRF impulses, the decrease in coronal-plane angular momentum is likely the result of the changes in vertical GRFs, consistent with previous results in straight-line walking (Silverman and Neptune, 2011), although foot placement may also have contributed. Future work should explore the mechanisms by which prosthesis stiffness affects whole-body angular momentum.

While this study identified the effects of prosthesis stiffness on walking mechanics and balance control during turning, there are some potential limitations. The prosthesis was modeled as a rigid body with a fixed axis of rotation for inverse dynamics calculations, which may have affected work calculations at the ankle. However, the same assumptions were made for all three stiffness levels and any associated bias would affect all three ankles similarly without altering relative differences between them. In addition, ankle stiffness levels remained constant across all subjects, whereas prescribed stiffness levels vary by body weight and activity level. The goal of the study was to test a systematic range of stiffness levels close to that which the amputees were prescribed, so this limitation was mitigated by recruiting only subjects who weighed less than 88 kg. Finally, the sagittal- and coronal-plane stiffnesses were coupled in this study, so the effects of stiffness in each plane could not be distinguished from those of the other. However, most energy storage and return feet have coupled sagittal- and coronal-plane stiffnesses by virtue of their design, so the conditions in this study reflect common clinical implementation.

In summary, many of the adaptations that occur with changes to sagittal-plane prosthesis stiffness in straight-line walking also occur during turning with concurrent changes in sagittal- and coronal-plane stiffness. Also, coronal-plane balance, as measured by the peak-to-peak range of angular momentum, improves with decreasing stiffness. However, adaptations in coronal-plane angles, work and GRF impulses were less systematic and more subject-specific than adaptations in the sagittal plane. Thus, while the effects of stiffness on turning mechanics must be evaluated for each individual, a more compliant prosthesis generally results in a more flexed leg, decreased body support, increased residual limb propulsion and improved balance.

Acknowledgements

The authors would like to thank Wayne Biggs, L/CPO, for aligning the study prostheses and Jan Pecoraro for help with subject recruitment. This study was supported by the National Science Foundation Graduate Research Fellowship Program (Grant DGE-1110007) and the

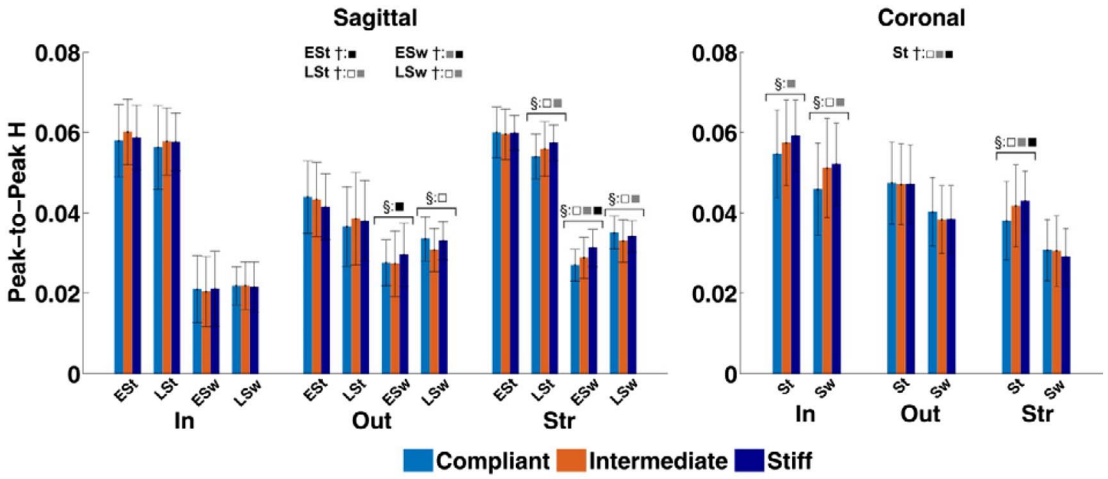

Fig. 5. Mean (standard deviation error bars) sagittal- and coronal-plane peak-to-peak range of whole-body angular momentum (H) normalized by subject mass and height for the residual limb on the inside (In) and outside (Out) of the turn as well as during straight-line walking at self-selected speed (Str) with the compliant, intermediate and stiff ankles. Sagittal-plane peak-to-peak range is shown for early stance (ESt), late stance (LSt), early swing (ESw) and late swing (LSw) while that in the coronal plane is divided into stance (St) and swing (Sw). Significant ankle main effects (†) as well as task∗ankle (§) interaction effects are indicated in addition to significant differences between the compliant and intermediate (□), compliant and stiff (■) and the intermediate and stiff (■) ankles.

U.S. Department of Veterans Affairs (Grant I01 RX000311).

Appendix A. Supplementary data

Supplementary data to this article can be found online at http://dx.doi.org/10.1016/j.clinbiomech.2017.08.003.

References

Curtze, C., Hof, A.L., Postema, K., Otten, B., 2012. The relative contributions of the prosthetic and sound limb to balance control in unilateral transtibial amputees. Gait Posture 36, 276–281.

Faustini, M.C., Neptune, R.R., Crawford, R.H., Rogers, W.E., Bosker, G., 2006. An experimental and theoretical framework for manufacturing prosthetic sockets for transtibial amputees. IEEE Trans. Neural Syst. Rehabil. Eng. 14, 304–310.

Faustini, M.C., Neptune, R.R., Crawford, R.H., Stanhope, S.J., 2008. Manufacture of passive dynamic ankle-foot orthoses using selective laser sintering. IEEE Trans. Biomed. Eng. 55, 784–790.

Fey, N.P., Klute, G.K., Neptune, R.R., 2011. The influence of energy storage and return foot stiffness on walking mechanics and muscle activity in below-knee amputees. Clin. Biomech. 26, 1025–1032.

Glaister, B.C., Bernatz, G.C., Klute, G.K., Orendurff, M.S., 2007. Video task analysis of turning during activities of daily living. Gait Posture 25, 289–294.

Glaister, B.C., Orendurff, M.S., Schoen, J.A., Bernatz, G.C., Klute, G.K., 2008. Ground reaction forces and impulses during a transient turning maneuver. J. Biomech. 41, 3090–3093.

Harper, N.G., Russell, E.M., Wilken, J.M., Neptune, R.R., 2014. Selective laser sintered versus carbon fiber passive-dynamic ankle-foot orthoses: a comparison of patient walking performance. J. Biomech. Eng. 136, 091001 (1-7).

Jenkyn, T.R., Shultz, R., Giffin, J.R., Birmingham, T.B., 2010. A comparison of subtalar joint motion during anticipated medial cutting turns and level walking using a multi-segment foot model. Gait Posture 31, 153–158.

Major, M.J., Twiste, M., Kenney, L.P.J., Howard, D., 2014. The effects of prosthetic ankle stiffness on ankle and knee kinematics, prosthetic limb loading, and net metabolic cost of transtibial amputee gait. Clin. Biomech. 29, 98–104.

Mattes, S.J., Martin, P.E., Royer, T.D., 2000. Walking symmetry and energy cost in persons with unilateral transtibial amputations: matching prosthetic and intact limb inertial properties. Arch. Phys. Med. Rehabil. 81, 561–568.

McConville, J.T., Churchill, T.D., Kaleps, I., Clauser, C.E., Cuzzi, J., 1980. Anthropometric relationships of body and body segment moments of inertia. Aerospace Medical Research Laboratory, Wright–Patterson Air Force Base, Dayton, Ohio.

Nederhand, M.J., Van Asseldonk, E.H.F., van der Kooij, H., Rietman, H.S., 2012. Dynamic balance control (DBC) in lower leg amputee subjects; contribution of the regulatory activity of the prosthesis side. Clin. Biomech. 27, 40–45.

Nott, C.R., Neptune, R.R., Kautz, S.A., 2014. Relationships between frontal-plane angular momentum and clinical balance measures during post-stroke hemiparetic walking. Gait Posture 39, 129–134.

Orendurff, M.S., Segal, A.D., Berge, J.S., Flick, K.C., Spanier, D., Klute, G.K., 2006. The kinematics and kinetics of turning: limb asymmetries associated with walking a circular path. Gait Posture 23, 106–111.

Pickle, N.T., Wilken, J.M., Aldridge, J.M., Neptune, R.R., Silverman, A.K., 2014. Whole-body angular momentum during stair walking using passive and powered lower-limb prostheses. J. Biomech. 47, 3380–3389.

Pijnappels, M., Bobbert, M.F., van Dieën, J.H., 2005. Push-off reactions in recovery after tripping discriminate young subjects, older non-fallers and older fallers. Gait Posture 21, 388–394.

Schrank, E.S., Stanhope, S.J., 2011. Dimensional accuracy of ankle-foot orthoses constructed by rapid customization and manufacturing framework. J. Rehabil. Res. Dev. 48, 31–42.

Schwartz, M.H., Rozumalski, A., 2005. A new method for estimating joint parameters from motion data. J. Biomech. 38, 107–116.

Segal, A.D., Orendurff, M.S., Czerniecki, J.M., Shofer, J.B., Klute, G.K., 2010. Local dynamic stability of amputees wearing a torsion adapter compared to a rigid adapter during straight-line and turning gait. J. Biomech. 43, 2798–2803.

Segal, A.D., Orendurff, M.S., Czerniecki, J.M., Schoen, J., Klute, G.K., 2011. Comparison of transtibial amputee and non-amputee biomechanics during a common turning task. Gait Posture 33, 41–47.

Sheehan, R.C., Beltran, E.J., Dingwell, J.B., Wilken, J.M., 2015. Mediolateral angular momentum changes in persons with amputation during perturbed walking. Gait Posture 41, 795–800.

Silverman, A.K., Neptune, R.R., 2011. Differences in whole-body angular momentum between below-knee amputees and non-amputees across walking speeds. J. Biomech. 44, 379–385.

South, B.J., Fey, N.P., Bosker, G., Neptune, R.R., 2010. Manufacture of energy storage and return prosthetic feet using selective laser sintering. J. Biomech. Eng. 132, 015001 (1-6).

Ventura, J.D., Klute, G.K., Neptune, R.R., 2011a. The effects of prosthetic ankle dorsiflexion and energy return on below-knee amputee leg loading. Clin. Biomech. 26, 298–303.

Ventura, J.D., Segal, A.D., Klute, G.K., Neptune, R.R., 2011b. Compensatory mechanisms of transtibial amputees during circular turning. Gait Posture 34, 307–312.

Zelik, K.E., Collins, S.H., Adamczyk, P.G., Segal, A.D., Klute, G.K., Morgenroth, D.C., Hahn, M.E., Orendurff, M.S., Czerniecki, J.M., Kuo, A.D., 2011. Systematic variation of prosthetic foot spring affects center-of-mass mechanics and metabolic cost during walking. IEEE Trans. Neural Syst. Rehabil. Eng. 19, 411–419.